UC Riverside

UC Riverside Previously Published Works

Title

The Latent Factor Structure Underlying Regional Brain Volume Change and Its Relation to Cognitive Change in Older Adults

Permalink

https://escholarship.org/uc/item/9kp099vm

Journal

Neuropsychology, 35(6)

ISSN

0894-4105

Authors

Gavett, Brandon E

Fletcher, Evan

Widaman, Keith F

et al.

Publication Date

2021-09-01

DOI

10.1037/neu0000761

Peer reviewed

eScholarship.org Powered by the California Digital Library
University of California

Author Manuscript

Author Manuscript

Author Manuscript

Author Manuscript

HHS Public Access

Author manuscript

Neuropsychology. Author manuscript; available in PMC 2022 September 01.

Published in final edited form as:

Neuropsychology. 2021 September ; 35(6): 643–655. doi:10.1037/neu0000761.

The Latent Factor Structure Underlying Regional Brain Volume Change and its Relation to Cognitive Change in Older Adults

Brandon E. Gavett[1], **Evan Fletcher**[2], **Keith F. Widaman**[3], **Sarah Tomaszewski Farias**[2], **Charles DeCarli**[2], **Dan Mungas**[2]

[1]School of Psychological Science, University of Western Australia

[2]Department of Neurology, University of California at Davis

[3]Graduate School of Education, University of California at Riverside

Abstract

Objective: Late-life changes in cognition and brain integrity are both highly multivariate, time-dependent processes that are essential for understanding cognitive aging and neurodegenerative disease outcomes. The current study seeks to identify a latent variable model capable of efficiently reducing a multitude of structural brain change magnetic resonance imaging (MRI) measurements into a smaller number of dimensions. We further seek to demonstrate the validity of this model by evaluating its ability to reproduce patterns of coordinated brain volume change and to explain rate of cognitive decline over time.

Method: We used longitudinal cognitive data and structural MRI scans, obtained from a diverse sample of 358 participants (M_{Age} = 74.81, SD = 7.17), to implement latent variable models for measuring brain change and to estimate the effects of these brain change factors on cognitive decline.

Results: Results supported a bifactor model for brain change with four group factors (prefrontal, temporolimbic, medial temporal, and posterior association) and one general change factor (global atrophy). Atrophy in the global (β = 0.434, SE = 0.070), temporolimbic (β = 0.275, SE = 0.085), and medial temporal (β = 0.240, SE = 0.085) factors were the strongest predictors of global cognitive decline. Overall, the brain change model explained 59% of the variance in global cognitive slope.

Conclusions: The current results suggest that brain change across 27 bilateral regions of interest can be grouped into five change factors, three of which (global gray matter, temporolimbic, and medial temporal lobe atrophy) are strongly associated with cognitive decline.

Keywords

Brain Mapping; Magnetic Resonance Imaging; Cognitive Aging; Longitudinal Studies; Factor Analysis, Statistical

Address correspondence to: Brandon Gavett, University of Western Australia (M304), 35 Stirling Highway, Perth, WA, 6009, Australia, brandon.gavett@uwa.edu.au.

Author Manuscript Author Manuscript Author Manuscript Author Manuscript

Understanding structural brain changes and their relations to cognitive decline are important goals in cognitive aging research (Mungas, Harvey, et al., 2005). One of the most common methods for measuring brain volume -- and changes in brain volume -- is structural magnetic resonance imaging (MRI). Structural MRI is capable of generating thousands of data points per individual at a single point in time. Despite the considerable advances in neuroimaging technology over the past several decades, many unanswered question remain about how to best aggregate and interpret structural brain changes when measured using MRI and how these changes are associated with cognitive decline in later life. The current study seeks to address these questions by (1) deriving a model for explaining coordinated brain volume changes across MRI-derived regions of interest (ROIs) and (2) using this model to explain parallel changes in cognitive functioning.

A number of previous studies have examined associations between structural brain changes and cognitive decline. Often, these studies have defined brain change using pre-selected ROIs, such as the hippocampus, entorhinal cortex, parahippocampal gyrus, orbitofrontal cortex, prefrontal cortex, cerebellum, white matter, lateral ventricles, and others (e.g., McArdle et al., 2004; Persson et al., 2016; Raz et al., 2005). Although such studies have undoubted value for elucidating the relations between regional brain volume changes and cognitive decline, defining brain change using a small number of pre-selected ROIs cannot fully address the fact that brain areas change together in coordinated ways (Carmichael et al., 2013). In fact, more comprehensive measurement of the coordinated patterns of volume change -- or lack thereof -- across among a large number of ROIs may lead to a better understanding of the processes underlying aging- and disease-associated brain changes (e.g., Iaccarino et al., 2018; Ossenkoppele et al., 2015). Such information about similarities and differences in regional brain atrophy rates may be difficult or impossible to glean when defining brain change on the basis of a small number of pre-selected ROIs. Further, ROIs that show statistically significant associations with cognitive decline in univariable models may no longer be significant when accounting for the variance explained by other ROIs in multivariable models (Fletcher et al., 2018).

However, making use of the vast quantity of data that is produced by structural MRI poses its own challenges. For instance, examining the associations between cognitive functioning and voxelwise brain volume measurements requires sophisticated statistical methods to properly handle the problem of multiple comparisons (Nichols & Holmes, 2002). As correcting for multiple comparisons is done to decrease the chances of making a Type I error, such corrections reduce statistical power and thus increase the chances of making a Type II error, potentially obscuring real associations between brain and cognition. Further, having more predictors in a model increases the chances of over-fitting the data, leading to results that are neither replicable nor useful for understanding brain-cognition associations (Mwangi, Tian, & Soares, 2014). Thus, a compromise is needed that can strike an appropriate balance between oversimplification and excessive complexity.

Latent variable methods for modeling brain change provide one such method of reaching this compromise. In particular, latent variable modeling allows for a large number of observed ROIs for brain change to be reduced into a smaller and more manageable number of latent brain change factors that explain the underlying patterns of change across the

Author Manuscript Author Manuscript Author Manuscript Author Manuscript

indicator ROIs. Such an approach can help to ensure that the variables used to define brain change are sufficiently comprehensive to provide a meaningful summary of coordinated atrophy, yet sufficiently parsimonious to minimize statistical issues related to multiple comparisons and statistical conclusion validity.

Three previous latent variable studies of brain change provide a particularly important background for the current study. Carmichael et al. (2013) identified a latent factor structure for explaining regional brain atrophy in participants with mild cognitive impairment (MCI) using exploratory structural equation modeling (SEM). Their results, obtained using MRI-derived Freesurfer ROI data from the Alzheimer's Disease Neuroimaging Initiative (ADNI) study, found evidence for five factors underlying changes in brain volume over time. Factor 1 was described as representing change in the default mode network, with the highest loadings on changes in the posterior cingulate cortex, precuneus, inferior parietal lobule, lateral temporo-parietal cortex, and the hippocampus. Factor 2 was interpreted to represent frontal cortex change, Factor 3 to represent atrophy in the medial temporal lobes, and Factor 4 to represent primary sensorimotor cortex atrophy. Finally, Factor 5 was largely representative of global brain change, as factor loadings were modest across all ROIs. These factors were found to predict risk of subsequent conversion to dementia, but the study did not evaluate the ability of the brain change factors to predict rate of change in cognition in a cognitively heterogeneous sample.

Fletcher and colleagues (2018) posited a hierarchical confirmatory factor analysis model with a global atrophy factor and orthogonal subfactors representing atrophy unique to the four lobes of the brain (frontal, temporal, parietal, and occipital, minus primary sensory and motor cortex). When modeled in conjunction with cognitive change over time, global gray matter atrophy was an important predictor of cognitive decline and temporal lobe change made an independent incremental contribution to cognitive decline above and beyond what could be explained by global gray matter atrophy (Fletcher et al., 2018). In a follow-up study, Gavett et al. (2018) extended this approach by examining differences due to race and ethnicity. They found evidence to suggest that the unique impact of temporal lobe atrophy on cognitive decline differs across ethnic and racial groups, with a stronger independent temporal atrophy contribution to cognitive decline in whites compared to blacks and Hispanics. In both the Fletcher et al. (2018) and Gavett et al. (2018) studies, regional brain atrophy factors were defined on the basis of the brain's major anatomical (lobar) divisions and may not provide the best representation of the coevolution of functionally relevant networks that span multiple lobes (e.g., the default mode network).

Thus, the current study seeks to build upon past work in this area by testing several possible models for explaining coordinated patterns of brain change, ranging from more lobar-based (e.g., Fletcher et al., 2018) to more network-based (e.g., Carmichael et al., 2013) to a hybrid approach based on functional cortical subtypes (e.g., Mesulam et al. 2000). This will be pursued in a sample of cognitively and demographically heterogeneous older adults who have undergone comprehensive neuropsychological assessment on a longitudinal basis. The goal of the current study is to identify a best-fitting factor model for cortical volume change that (1) fits brain ROI change variables well, thus reducing these cortical ROIs to a smaller number of factors that capture important functional differences in regional brain atrophy, and

Author Manuscript Author Manuscript Author Manuscript Author Manuscript

(2) fits well in the context of longitudinal cognitive data, thus helping us better understand how the identified brain change factors relate to aging-associated cognitive decline across the spectrum of cognitive health from cognitively intact to dementia.

Method

Participants

The University of California Davis (UCD) Aging Diversity Cohort provided the study sample. This is a longitudinal study of cognitive aging in an educationally, ethnically, and cognitively diverse cohort of older adults. This cohort approximates the diverse racial, ethnic, and socioeconomic composition of a six-county catchment area in the central Sacramento/San Joaquin valley and east San Francisco Bay area of Northern California. It is composed of Hispanic/Latinx, Black/African American, and non-Hispanic White/Caucasian participants, has wide variability in educational attainment, and spans the spectrum of cognitive function from normal to dementia. About two-thirds of this cohort were recruited through a community screening program that was designed to recruit community dwelling individuals without regard to their level of cognitive function; that is, to represent the range and distribution of cognitive function in the community. The other one-third were initially seen for clinical evaluation at a university memory/dementia clinic and referred for research. Cohort composition and recruitment methods are described in Hinton et al. (2010).

Participants were 358 persons who had received at least two cognitive evaluations and at least two MRI brain scans. There were 170 white, 90 Hispanic, 79 black, and 19 participants reporting other ethnic/racial identity. The majority (n = 310, 87.1%) were tested in English, and the remainder were tested in Spanish. Approximately two-thirds of the Hispanic participants reported Mexican ancestry. The community screening program identified 273 individuals, whereas 85 were clinical referrals.

Participants were evaluated and followed within the research program of the UCD Alzheimer's Disease Center (ADC). Enrollment began in 2001 and a rolling enrollment design was used to build the cohort with substantial enrollment continuing through 2010. All participants in this study had at least two cognitive evaluations and at least two MRIs but, due to rolling enrollment, there was variability in the total number of evaluations completed by each participant. Inclusion criteria for the longitudinal cohort included age 60 or older at their first examination and ability to speak English or Spanish. Exclusion criteria included unstable major medical illness, major primary psychiatric disorder, and substance abuse or dependence in the last five years. Participants received clinical evaluations through the UCD ADC on a roughly annual basis that included consensus diagnosis, based on standard diagnostic criteria (e.g., Albert et al., 2011; McKhann et al., 1984; McKhann et al., 2011; Winblad et al., 2004), of normal cognition versus MCI versus dementia as well as etiologic diagnosis. All participants provided informed consent, and all human subject involvement was in accordance with the Declaration of Helsinki as overseen by institutional review boards at the University of California at Davis, the Veterans Administration Northern California Health Care System, and San Joaquin General Hospital in Stockton, California. Data used in this manuscript are available via a request to the authors and require a data use agreement between institutions. Code used in this manuscript is available upon request.

Author Manuscript Author Manuscript Author Manuscript Author Manuscript

MRI Measures

Structural T1-weighted MRI scans were acquired by the UCD ADC. We used subjects having at least two scans, with an interscan interval greater than one year, in order to obtain robust measurements of longitudinal change (see below). The majority (68%) were made from 1.5T scanners at both time points, mainly using GE Genesis Signa, but some Philips Eclipse. A few (about 5%) were 3T scans at both acquisitions, using Siemens TimTrio; a larger fraction had 1.5T at the earlier scan and 3T at the later scan, and a few scans were unidentified.

MRI measurements were computed as part of our in-house processing pipeline described in previous studies (e.g., Fletcher, 2014; Lee et al., 2010). Briefly, structural T1-weighted MR images were processed to remove the skull (i.e., skull-stripped) using an atlas-based method (Aljabar, Heckemann, Hammers, Hajnal, & Rueckert, 2009) followed by human quality control to provide generally minor cleanup if needed. The skull-stripped structural T1-weighted MR brain images were then nonlinearly registered to a minimal deformation template (MDT) synthetic brain image (Kochunov et al., 2001) adapted for an age range of 60 and above; the registration was performed by a cubic B-spline deformation (Rueckert, Aljabar, Heckemann, Hajnal, & Hammers, 2006). Registration parameters were stored for later use to place our atlas-based ROI masks onto native space T1-weighted skull-stripped brain images, and for initializing the tissue segmentation of those native images.

Four-tissue segmentation of native space stripped T1-weighted brain images was performed in two steps. We first computed three-tissue cerebrospinal fluid, gray matter and white matter segmentations using an automatic tissue class initialization from our segmented template, followed by iterated alternating voxel class assignment and tissue class parameter estimation until convergence, in an algorithm designed to enhance accuracy at likely tissue boundaries (Fletcher, Singh, Harvey, Carmichael, & DeCarli, 2012). Segmentation for white matter hyperintensity lesions was then added using intensity-normalized native space fluid-attenuated inversion recovery (FLAIR) images previously aligned to the native space structural T1s via an in-house pipeline (DeCarli, Maillard, & Fletcher, 2013). In this approach, white matter hyperintensity lesions are computed from hyperintense FLAIR values that lie strictly within previously segmented white matter, thus avoiding gray matter-white matter boundaries (DeCarli et al., 2013). Finally, native gray matter ROI volumes were computed by reverse transforming MDT ROI masks into native space using the B-spline registration parameters via an in-house application using trilinear interpolation. To address the issues of partial voluming (i.e., non-binary values) at mask boundaries, all ROI masks were deformed in one pass, followed by a voting scheme to assign each native gray matter voxel to the ROI for which the deformed mask intensity was the highest. This also ensured that our cortical parcellations lay only within gray matter. The ROIs were 31 bilateral regions derived from the Mindboggle atlas (Klein & Tourville, 2012) plus a bilateral hippocampus ROI derived from atlas-based segmentation in native space (Aljabar et al., 2009).

We computed native space longitudinal structural brain change in each subject via registration of a single pair of repeat scans having the most widely separated time points greater than one year. We used a tensor-based morphometry (TBM) method designed

Author Manuscript Author Manuscript Author Manuscript Author Manuscript

to enhance sensitivity and specificity for biological change by incorporating estimates of likely tissue boundaries (Fletcher, 2014; Fletcher et al., 2013). TBM generates deformation fields registering brain scans at differing time points and uses these to estimate local volume changes between the scans (Ashburner & Friston, 2000). This processing was done via an in-house processing pipeline that has been previously described (Fletcher et al., 2016). Image pre-processing included intensity inhomogeneity correction followed by linear alignment and resampling of each image to a "halfway space" in order to equalize voxel interpolation levels (Mak et al., 2015), which otherwise might make edges in one image appear stronger or displaced relative to the other. The log-transformed determinant of the 3×3 Jacobian matrix of the TBM deformation at each voxel (i.e. log-Jacobian) quantifies local, voxel-based brain change. Atrophy rates were annualized to represent a uniform interscan period for all subjects. Regional tissue change rates for gray matter ROIs were computed in native space as log-Jacobian means in each native ROI gray matter volume.

Cognitive Assessment

The cognitive outcomes in this study were composite measures of episodic memory, semantic memory, executive function, and spatial ability derived from the Spanish and English Neuropsychological Assessment Scales (SENAS). The SENAS has undergone extensive development as a battery of cognitive tests relevant to cognitive aging that allow for valid comparisons across race/ethnic groups (Mungas, Reed, Marshall, & González, 2000; Mungas, Reed, Crane, Haan, & González, 2004; Mungas et al., 2005a, 2005b). The episodic memory composite score is derived from a multi-trial word-list-learning test (Mungas et al., 2004). The semantic memory composite is derived from highly correlated verbal (object-naming) and nonverbal (picture association) tasks. The executive function composite is constructed from component tasks of category fluency, phonemic (letter) fluency, and working memory (digit-span backward, visual-span backward, list sorting). Spatial ability is measured using the SENAS Spatial Localization scale, which assesses ability to perceive and reproduce two-dimensional spatial relationships that are increasingly complex. These measures were administered at all evaluations. Language of test administration was determined by an algorithm that combined information regarding each participant's language preference in several specific contexts (e.g., conversing at home, listening to radio or television, conversing outside the home, preferred language for reading). Administration procedures, measure development, and psychometric characteristics of the SENAS battery are described in more detail elsewhere (Mungas et al., 2004).

Data Analysis

Overview of our approach.—Data analysis consisted of three steps. First, we built confirmatory factor analytic models for brain change and examined the ability of these factors to reproduce patterns of brain atrophy across approximately 32 ROIs (the exact number differs by model). Second, we used latent growth curve modeling to understand patterns of cognitive change on the four SENAS domains independent of the brain change modeling performed in step 1. Finally, in the third step, we integrated the brain change models from step 1 with the cognitive change models in step 2. We sought to identify the integrated brain change/cognitive change model that best fit the data and, subsequently, to

Author Manuscript Author Manuscript Author Manuscript Author Manuscript

identify the brain change factors from these models that were best able to predict cognitive change.

Data analysis was performed using Mplus version 8.1 (Muthén & Muthén, 1998). Fit statistics for each model were obtained using a robust maximum likelihood estimator that used full information maximum likelihood to handle missing data. The suitability of model fit to the data was judged using the comparative fit index (CFI), Tucker-Lewis Index (TLI), root mean square error of approximation (RMSEA) and its 90% confidence interval, and standardized root mean square residual (SRMR). Standard criteria for judging goodness of fit were used to ensure that the models being compared provided reasonably good fit to the data, and these model fit statistics were also used to compare models with one another (Hu & Bentler, 1999). Parameter estimates and their 95% highest density intervals (HDI) were derived using Bayesian estimation.

Measurement models for brain change.—A series of competing measurement models for brain change were examined. We specified a network-based model (Model 1), inspired by Carmichael et al., (2013), as a bifactor model with group factors representing Factors 1–4 and an orthogonal global factor representing Factor 5. Because this model produced a “not positive definite” latent variable covariance (psi) matrix error due to an estimated correlation of > 1 between factors 1 (default mode network) and 3 (medial temporal lobes), we combined these two factors into a single factor in our analyses. The lobar-based model (Model 2) was inspired by Fletcher et al. (2018), and included primary sensory and motor cortex ROIs and limbic system ROIs. Whereas Fletcher et al. (2018) used four less-granular lobar ROIs (frontal, temporal, occipital, and parietal) as indicators of brain change, the current study employed 32 more granular ROIs as indicators of global brain change and of regional change in the brain’s four lobes (e.g., volume change in the middle temporal gyrus ROI was an indicator both of global brain change and of a specific temporal lobe change factor).

Model 3 was developed with consideration of different functional cortical subtypes (e.g., Mesulam et al., 2000), represented by a global brain change factor and four group factors representing volume changes unique to prefrontal association cortex, temporolimbic (i.e., temporal lobe neocortex, insula, and cingulate gyrus), medial temporal lobe (i.e., hippocampus, entorhinal cortex, and parahippocampal gyrus), and posterior association cortex. This model excluded primary sensory and motor cortex, based on evidence suggesting these areas are often spared from the most pronounced effects of neurodegeneration and contribute less to higher level cognitive skills (e.g., Braak, Braak, & Bohl, 1993; Mesulam, 2000).

Finally, we designed a fourth model to represent a single-factor structure for brain change indicated by all ROIs (Model 4). This model was not hypothesized to fit the brain change data as well as the other three models, but was included as a reference for comparison purposes.

Throughout, all brain change measurement models were parameterized by fixing the factor variances to 1 and freely estimating the factor loadings of the first indicators of each latent

Author Manuscript Author Manuscript Author Manuscript Author Manuscript

factor. The brain change group factors were allowed to covary regardless of whether a bifactor structure was used to model global brain change. However, when a bifactor structure was used, the global factor's correlations with the group factors were always fixed to 0. As in Carmichael et al. (2013), our models included residual covariance terms to account for shared error variance caused by imprecise boundary placement of adjacent ROIs in atlas-based parcellation methods.

Measurement models for cognitive change.—Four indicators of cognitive functioning were obtained from the longitudinal neuropsychological assessments of each cognitive domain; these measures of verbal episodic memory, semantic memory, spatial skills, and executive functioning were captured at approximately annual intervals. We modeled change in cognitive functioning using four different linear latent growth curve models, with the intent of proceeding with the best fitting model from the following: (1) separate intercepts/separate slopes; (2) separate intercepts/global slope; (3) global intercept/separate slopes; and (4) global intercept/global slope. In the current study, we used cognitive data from up to eight annual study visits, as this length of follow-up was the longest we could include before encountering warnings related to low covariance coverage.

Structural models for estimating brain change effects on cognitive change.—After analyzing four potential measurement models for brain change in the first stage and four measurement models for cognitive change in the second stage, the best-fitting cognitive model was integrated with each of the brain change models so that the brain change and cognitive change components could be estimated simultaneously. All models included the following covariates, onto which the separate cognitive intercepts and global cognitive slope were regressed: sex (reference = female), years of education (centered at 12), age at baseline (centered at 70 years), and recruitment source (reference = community). This allowed us to estimate the effects of brain change on cognitive change, above and beyond the effects of covariates, in order to identify the brain change factors that are the most important contributors to global cognitive decline. These four integrated models were examined for goodness of fit and also for the parameter estimates regressing global cognitive slope onto brain change factors. Although we allowed the brain change factors and the four separate cognitive intercepts to freely correlate, the parameter estimates for these correlations were not a focus of our interpretation.

Results

Participant baseline demographics and other descriptive data are shown in Table 1. Participants were most commonly diagnosed as cognitively normal at baseline, but a sizeable proportion of the sample was diagnosed with MCI and a minority with dementia. Baseline cognitive test scores and dementia severity measures were largely consistent with that composition.

Measurement Models for Brain Change

First, we examined model fit of our four hypothesized brain change models in the absence of cognitive data. Three of these four models had a bifactor structure with a global brain

Author Manuscript Author Manuscript Author Manuscript Author Manuscript

change factor and multiple group factors. The one exception was the single factor model (Model 4). Table 2 provides more detail about each model, including the factors modeled and their brain change ROI indicators.

Of the four brain change models reported here, Model 3 produced the best fit (CFI = 0.95, TLI = 0.924, RMSEA = 0.065, SRMR = 0.037). Comprehensive model fit statistics are provided in Supplementary Table 1.

Measurement Models for Cognitive Change

Consistent with previous findings (Fletcher et al., 2018; Gavett et al., 2018; Mungas et al., 2018), the best fitting model to the cognitive change data used separate intercepts and a global slope (Supplemental Table 2). This growth model was therefore combined in subsequent analyses – along with covariates – with the four brain change measurement models described above, allowing the global slope to serve as the primary outcome variable that was regressed onto the identified brain change factors.

Structural Models for Estimating Brain Change Effects on Cognitive Change

When comparing the fits of the structural models combining both brain change and cognitive change, Model 3 provided the best fit to the data (Table 3). Therefore, the results presented in the following sections are based on that model.

Sensitivity Analysis

One of the brain change group factors (prefrontal) in Model 3 was highly collinear with two of the other group factors (temporolimbic, $r = 0.913$, 95% HDI [0.878, 0.941]; posterior association, $r = 0.898$, 95% HDI [0.856, 0.932]). When all of these brain change group factors are used together as predictors, this multicollinearity may lead to biased parameter estimates for the regressions of cognitive change on brain change. Given the potential impediment caused by this multicollinearity for interpreting brain change effects on cognitive change, we ran a series of univariable (plus covariates) models examining the strength of association between the brain change factors in Model 3 and cognitive change, one brain change predictor at a time. In univariable models, all brain change factors were strong predictors of cognitive change (global brain, $\beta = 0.44$, SE = 0.07; medial temporal, $\beta = 0.43$, SE = 0.07; prefrontal, $\beta = 0.28$, SE = 0.07; temporolimbic, $\beta = 0.45$, SE = 0.06) except the posterior association change factor ($\beta = 0.14$, SE = 0.08).

These univariable analyses were followed by multivariable analyses. By systematically varying which brain change factors were treated as predictors, we found that a model treating global brain, temporolimbic, and medial temporal change factors as predictors of cognition – and prefrontal and posterior association change factors as simply correlated with cognition – addressed the problem of multicollinearity and led to more trustworthy estimates of the effects of brain change on cognitive change. The results of these model comparisons are shown in Supplemental Table 4. This model was then subjected to a second sensitivity analysis, described below.

Author Manuscript Author Manuscript Author Manuscript Author Manuscript

For the second sensitivity analysis, we manipulated the absence (i.e., orthogonality) or presence (i.e., non-orthogonality) of shared variance between (a) the residuals of adjacent brain regions with one another and (b) the brain change group factors with one another. We sought to determine whether these manipulations affected model fit and whether the regression parameter estimates were robust to these changes in model parameterization. The model generated using our initial approach (allowing adjacent ROIs to share residual covariance and allowing group factors to correlate with one another) provided the best fit to the data. A model that did not allow adjacent ROIs to share residual covariance and constrained the group factors to be orthogonal to one another produced a "not positive definite" error. A comparison of the model fit statistics for each of the models examined is shown in Supplemental Table 5. Standardized regression parameter estimates, shown in Supplemental Table 6, varied depending on the model, but maintained the same relative order of effect size magnitude (global brain change > temporolimbic > medial temporal) in each model.

The model that performed best after these sensitivity analyses is depicted graphically in Figures 1 and 2. Figure 1A provides a schematic showing how residual covariances between adjacent ROIs were modeled, the factors for which each ROI serves as an indicator (color-coding), as well as with the magnitude (edge weights) and sign (dashed edges = negative; no edges = non-adjacent) of these residual covariances. Figure 1B shows a path diagram representing the hypotheses tested in the structural model regressing global cognitive slope on the brain change factors. Figure 2 shows a 3D surface map color-coded to illustrate the four brain change group factors derived from the most preferred model (Model 3).

The standardized factor loadings of the 27 ROIs in this model onto the five latent factors are shown in Table 4. In this model, global cognitive decline was more rapid in clinic versus community referrals ($\beta = -0.700$, 95% HDI [−0.922, −0.470]), but did not differ by sex ($\beta = -0.015$, 95% HDI [−0.211, 0.178]), education ($\beta = 0.060$, 95% HDI [−0.032, 0.150]), or age ($\beta = -0.029$, 95% HDI [−0.127, 0.066]). Other parameter estimates from this model, presented in Table 5, reveal that the global brain, temporolimbic, and medial temporal change factors were all strong predictors of global cognitive change. Together, the predictor variables used in Model 3 were able to explain 59.2% (95% HDI [49.0%, 69.4%]) of the variance in global cognitive slope.

Discussion

In this study, we executed a systematic approach to modeling (1) coordinated volume changes in cortical gray matter ROIs, (2) longitudinal changes in four cognitive domains, and (3) the effects of concomitant changes in brain ROI volumes on global cognitive change. Although these approaches themselves are not novel, a major strength of this study is the full integration of brain ROI and cognitive change data within the same modeling framework, in a cognitively and demographically heterogeneous sample of older adults, over a long period of follow-up (8 visits), using a comprehensive and well-validated neuropsychological assessment battery. Consequently, we identified a latent variable model that provides good fit to observed changes in brain volume across ROIs and fits well when used to predict longitudinal cognitive outcomes. This model, shown in Figure 1, represents the best

Author Manuscript Author Manuscript Author Manuscript Author Manuscript

combination of being substantively meaningful, reproduces the covariance of brain change ROIs, and explains almost 60% of the variance in cognitive decline. The results of this study reveal that hippocampus and Mindboggle ROI volume changes can be used as manifest indicators of latent prefrontal, posterior association, medial temporal, and temporolimbic brain change factors – along with a global brain change factor that is orthogonal to the correlated group factors – that explain rate of global cognitive decline.

These results suggest the presence of five dissociable components of brain atrophy that exert differential effects on cognitive decline in older adults. The presence of the specific group factors indicates that volume changes in the temporal lobe neocortex plus several limbic system structures (subcomponents of the cingulate gyrus and insula) were dissociable from volume changes in medial temporal lobe structures (hippocampus, entorhinal cortex, and parahippocampal gyrus), in terms of both shared variance in atrophy rates and influence on cognitive decline. Also dissociable were volume changes in the prefrontal cortex and posterior association cortex. The parameter estimates derived from the optimal Model 3 indicate that – when holding other predictor variables constant – a 1 SD annual decline in global gray matter volume is associated with an expected reduction of 0.43 SD per year in global cognition (Table 5). Similarly, for every 1 SD of annual decline in temporolimbic volume, global cognition is expected to decline by 0.28 SD per year, and for every 1 SD of annual decline in medial temporal lobe volume, global cognition is expected to decline by 0.24 SD per year (Table 5). These results are largely consistent with our previous work on brain change and cognitive decline showing that global brain atrophy and the incremental contribution of temporal lobe atrophy are the strongest predictors of cognitive decline (Fletcher et al., 2018; Gavett et al., 2018).

Most of the group factors were highly correlated, especially the prefrontal factor with the posterior association and temporolimbic factors. However, there was value in separating these three factors, both in terms of model fit (a model combining these factors into one did not fit the data as well; data not shown) and in terms of explaining cognitive decline. Even though the temporolimbic change factor was highly correlated with the prefrontal change factor, the value in modeling these factors separately is evident from the temporolimbic factor's stronger association with cognitive decline (see Table 5 and Supplemental Table 4). And even though the prefrontal and posterior association change factors were highly correlated with one another and were both better modeled as being correlated with – rather than predictive of – global cognitive slope, a model combining these two factors into one also led to a decrement in model fit (data not shown). The correlations between the medial temporal change factor and the other group factors were more modest, and a separate medial temporal factor offered incremental predictive validity for cognitive decline.

In addition to the research reviewed above, other studies have also attempted to divide the brain into meaningfully dissociable regions that relate to cognitive change. For instance, Zhang et al. (2016) took an exploratory approach, using voxel based morphometry applied to cross-sectional gray matter thickness as a proxy for brain atrophy and Bayesian latent Dirichlet allocation (Blei, Ng, & Jordan, 2003) to identify latent factors for gray matter thickness. Based on their analysis of a sample of participants with Alzheimer's disease, Zhang et al. (2016) identified three brain factors, which they labeled cortical (including

Author Manuscript Author Manuscript Author Manuscript Author Manuscript

frontal, lateral temporal, parietal, and lateral occipital), temporal (medial temporal cortex, hippocampus, and amygdala), and subcortical (striatum, thalamus, and cerebellum). In a sample of amyloid-positive MCI participants and cognitively normal individuals, episodic memory was closely linked to the temporal factor, executive functioning was closely linked to the cortical factor, and cognitive performance was not strongly related to the subcortical factor.

Our findings were consistent with Zhang et al. (2016) in that we found temporal lobe atrophy to be strongly and differentially predictive of cognitive decline beyond the effects of global brain atrophy (Table 5). The current results extend those reported by Zhang et al. (2016) by differentiating temporal effects into temporolimbic and MTL factors, consistent with other prior findings (Fjell, McEvoy, Holland, Dale, & Walhovd, 2014; Fjell et al., 2009). We have also built on the work of Zhang et al. (2016) by examining the degree to which our identified brain change factors relate to cognitive change, and by studying these relations across the entire spectrum of cognitive health from cognitively intact to dementia. As such, our results can be generalized to a broad range of brain and cognitive health, rather than just the later stages.

Methodological differences make it difficult to directly compare our results to other studies that motivated this work. For example, Carmichael et al. (2013) did not examine longitudinal cognitive trajectories, Zhang et al. (2016) examined decline in memory and executive functioning as separate outcomes of cross-sectional gray matter factors as proxies for atrophy, and both studies relied on data-driven (i.e., exploratory) approaches to identify their brain change factors. Nevertheless, some consistent patterns emerged across studies. Carmichael et al. (2013) identified a default mode network factor (which included numerous temporal lobe and limbic system ROIs) and a separate medial temporal lobe change factor, both of which were good predictors of future dementia risk. Similarly, Zhang et al. (2016) reported temporal lobe effects on decline in episodic memory. Thus, across studies employing different methods in different samples, there is converging evidence that (a) factors heavily influenced by atrophy in temporolimbic and medial temporal lobe structures are statistically distinguishable from factors influenced by atrophy in other brain regions, and (b) greater atrophy in these temporal-centric factors is associated with more negative cognitive outcomes.

Also consistent with our previous work is the finding that prefrontal and posterior association atrophy is not strongly predictive of cognitive decline when accounting for global and temporal lobe atrophy (Fletcher et al., 2018). In all univariable models, individual brain atrophy factors predicted cognitive decline in the expected direction. In multivariable models, however, the prefrontal and posterior change factors were negatively and weakly correlated with global cognitive slope in the context of other covariates. This seemingly counterintuitive finding may be related to the high correlations between the prefrontal change, posterior association change, and temporolimbic change factors (Table 5). These negative associations with cognitive change, in the context of the overall model, suggest that cognitive decline may be more rapid when the frontal and posterior areas undergo relatively *less* atrophy than would be expected on the basis of global gray matter change, temporolimbic change, and medial temporal change. This pattern is consistent with the

Author Manuscript Author Manuscript Author Manuscript Author Manuscript

commonly observed effects of AD, where neuropathological changes accumulate in the medial temporal lobes and other temporolimbic areas early in the disease course (Braak & Braak, 1991; 1996). Holding global gray matter atrophy constant, disproportionately greater atrophy in the temporolimbic and medial temporal areas, relative to atrophy in the frontal and posterior association areas, is directly related to the rate at which cognitive decline is expected to occur. To summarize: when viewed in isolation (i.e., in univariable models) prefrontal and posterior association atrophy rates are each positively associated with cognitive change. However, when viewed in the context of dominant medial temporal and temporolimbic atrophy (i.e., in multivariable models), their associations became negative, reflecting the relatively stronger effects of medial temporal and temporolimbic atrophy on cognitive decline.

These findings have clinical and diagnostic relevance. For example, previous evidence has suggested that AD can be divided into three pathological subtypes: typical (relatively uniform neuropathological changes across the limbic system and neocortical association areas), hippocampal sparing (disproportionately greater atrophy of neocortical association areas compared to the medial temporal lobes), and limbic predominant (disproportionately greater atrophy of the medial temporal lobes compared to neocortical association areas; Murray et al., 2011; Whitwell et al., 2012). At times, a fourth subtype, minimal atrophy, has also been described (Byun et al., 2015; Persson et al., 2017). By providing quantitative estimates of brain atrophy in global gray matter and specific medial temporal, temporolimbic, prefrontal, and posterior association ROIs, the latent brain change factors in the current study are capable of reproducing these AD subtypes.

One strength of our study is that the identified factor structure was based on a cognitively heterogeneous sample ranging from cognitively normal to dementia, thus allowing us to capture broad variability in our continuous predictors and outcomes. Nevertheless, AD and cerebrovascular pathology were the most common causes of MCI and dementia in the current sample. Additional research is needed to determine whether the factor structure identified here can be replicated in samples with both similar and different etiologic compositions. For example, future replication in samples composed of individuals with similar suspected neuropathology to the current sample would provide greater confidence in the generalizability of these results. In addition, replication in samples containing individuals with other neurodegenerative conditions, such as dementia with Lewy Bodies and frontotemporal lobar degeneration, would allow for inferences to be made about whether the brain-behavior change relationships observed here are specific to AD and cerebrovascular pathology, or if they apply more broadly in the context of other causes of neurodegeneration. To cite one possibility, in samples containing a higher prevalence of frontotemporal dementia, posterior cortical atrophy, or limbic-predominant age-related TDP-43 encephalopathy, different patterns of association may emerge between cognitive decline and the prefrontal, posterior association, and medial temporal change factors, respectively. Future research extending the current findings may seek to evaluate this model across different subgroups, defined by clinical diagnosis, suspected etiology, or racial/ethnic background.

Author Manuscript Author Manuscript Author Manuscript Author Manuscript

Other strengths of this study include the use of a confirmatory approach to specifying the model's factor structure, the psychometrically sophisticated and comprehensive neuropsychological test battery, the availability of seven years of neuropsychological outcome data, and a diverse cohort broadly representative of both community and clinic populations. Also, our use of a Bayesian approach to model estimation and derivation of 95% highest density credible intervals, along with the sensitivity analyses designed to explore alternative approaches to model parameterization, provide confidence that our conclusions are not based on spurious findings or problems related to multiple comparisons. Our analyses provided a rigorous and thorough test of several alternative approaches to the factor structure and model parameterization. Given the complexity of these models, we performed sensitivity analyses to ensure that alternative approaches to model parameterization were explored. Although these modifications help ensure the robustness of our results, they can also increase the potential to capitalize on sample-specific patterns in the data, thus reinforcing our earlier statement that independent replication is warranted.

This research may be limited by our choice to study volume changes in bilateral ROIs together, rather than separated by hemisphere. In other words, there may be hemispheric differences in the patterns by which brain ROIs undergo coordinated volume changes, and these potential asymmetries may differentially affect cognition. Similarly, we made the decision to use only cortical, not subcortical, ROIs in our analysis. Our choice to restrict our analyses to bilateral cortical ROIs was largely based on three factors: (1) a desire to maintain consistency with the approaches used by Carmichael et al. (2013) and Fletcher et al. (2018); (2) practicality, as the addition of dozens of additional brain ROI variables to the model would have markedly increased the complexity of an already complex set of analyses; and (3) the Zhang et al. (2016) study did not provide evidence of a strong association between subcortical ROIs and cognitive functioning. Nevertheless, the current results can provide a jumping off point for further research seeking to examine lateralized differences in brain atrophy rates and their relations to cognitive change.

Further, the use of an ROI parcellation map altogether may also be seen as a limitation. Any model derived from ROIs must assume that inter-ROI boundary differences are meaningful, but that intra-ROI differences are not. Such a morphometric way of parcellating the brain is becoming increasingly inconsistent with known models for how the brain functions. Functional connectivity studies, graph network theory, and similar approaches have identified functional networks in the brain that cannot be faithfully reproduced using cortical ROIs alone (Bassett & Bullmore, 2017; VandenHeuvel & Sporns, 2011). One reason for this is that some of these functional networks include subcortical structures (e.g., amygdala, basal ganglia) that may not be routinely derived from some parcellation maps. Another reason for this lack of fidelity is that large scale distributed networks may require more granular distinctions between cortical regions than is available in some cortical parcellation atlases. For example, modeling atrophy in the dorsal attention network (Vossel, Geng, & Fink, 2014) requires ROIs for the frontal eye field and inferior parietal sulcus, which are not separable from surrounding tissue using the Mindboggle or similar atlases (Vernet, Quentin, Chanes, Mitsumasu, & Valero-Cabré, 2014). Optimal factor models for explaining coordinated regional brain atrophy may require different indicators – network

Author Manuscript Author Manuscript Author Manuscript Author Manuscript

based, in addition to morphometric based – of the underlying brain change factors than those used here.

It is also important to address the issue of different scanner field strengths used for our longitudinal computations. Although a majority (73%) of our sample had the same field strengths for both time points, we decided that inclusion of the other subjects with differing scan strengths was warranted, on the basis of the improved statistical power it offered. Since 3T images may have somewhat sharper edges, the possible cost would be increased inconsistencies in the log-Jacobian change maps of subjects with mixed field strengths, but we believe this risk is minimal. As explained above in the MRI measures section of the methods, our in-house TBM computations incorporate statistical edge detection features to help reduce uncertainties in the locations of edges driving the deformations (Fletcher et al., 2013, Fletcher 2014), The preprocessing steps outlined above, including inhomogeneity correction and halfway space coregistration, also minimize sensitivity to differences in image edges.

The results of this study reveal that, in older adults, regional brain atrophy follows a coordinated pattern that can be summarized by global cortical atrophy plus atrophy unique to the temporolimbic region, medial temporal lobes, prefrontal association cortex, and posterior association cortex. Further, rates of global cortical atrophy, temporolimbic atrophy, and medial temporal lobe atrophy can -- in combination with demographic covariates -- explain approximately 60% of the variance in cognitive decline, which is a very large and clinically meaningful effect. The current study makes several important contributions to the literature. First, there are few, if any, studies that have validated *a priori* hypotheses about the factor structure underlying coordinated brain change across a large number of ROIs (over two dozen), inclusive of both neocortical and limbic system regions. Second, studies examining the associations between a comprehensive model of brain change and a comprehensive model for cognitive change are rare. Our study builds upon existing research by validating a brain change factor model against a psychometrically sophisticated neuropsychological test battery composed of four cognitive abilities measured over a lengthy period of time (8 years). Third, the results presented here were obtained in a sample that demonstrates diversity across a variety of dimensions, including race/ethnicity, degree of cognitive impairment, and referral source (clinic and community referrals are both well-represented). Other studies investigating changes in brain-cognition associations have been variously limited by a small number of brain regions, less comprehensive cognitive outcomes, limited cognitive heterogeneity, or samples with limited demographic diversity. Given the strengths of this study, the model reported here can serve as a foundation for additional research investigating changes in brain-cognition associations that occur as a result of aging and neurodegenerative disease processes. Future studies can expand upon these results by incorporating increased etiologic diversity and by incorporating additional predictors, mediators, moderators, and outcome variables, to more fully capture the complex associations between brain change and cognitive decline in older adults.

Supplementary Material

Refer to Web version on PubMed Central for supplementary material.

Author Manuscript Author Manuscript Author Manuscript Author Manuscript

Acknowledgments

This work was supported by multiple grants from the National Institute on Aging (P30 AG10129, R01 AG021028, and R01 AG047827, C.D., PI; R01 AG10220, D.M., PI; R01 AG031563, D.M., PI; R01 AG031252, S.T.F., PI). Analysis and article development were supported by a National Institute on Aging Resource Centers for Minority Aging Research grant (P30 AG043097, L Hinton, PI).

The data that support the findings of this study are available from the University of California, Davis Alzheimer's Disease Center. Restrictions apply to the availability of these data. Requests for data access can be made to the senior author (DM) at dmmungas@ucdavis.edu and may be subject to a data use agreement.

We would like to acknowledge the devotion of the participants in this study, who volunteered their time for comprehensive annual evaluations and repeated MRI scans. Many staff of the UC Davis Alzheimer's Disease Center made this study a reality. Esther Lara supervised all aspects of study implementation from participant recruitment through retention over time leading to successful longitudinal follow-up.

References

Akaike H (1987). Factor analysis and AIC. Psychometrika, 52(3), 317–332. doi:10.1007/BF02294359

Albert MS, DeKosky ST, Dickson D, Dubois B, Feldman HH, Fox NC, … Phelps CH (2011). The diagnosis of mild cognitive impairment due to Alzheimer's disease: Recommendations from the National Institute on Aging-Alzheimer's Association workgroups on diagnostic guidelines for Alzheimer's disease. doi:10.1016/j.jalz.2011.03.008

Aljabar P, Heckemann RA, Hammers A, Hajnal JV, & Rueckert D (2009). Multi-atlas based segmentation of brain images: Atlas selection and its effect on accuracy. NeuroImage, 46(3), 726–738. doi:10.1016/j.neuroimage.2009.02.018 [PubMed: 19245840]

Ashburner J, & Friston KJ (2000). Voxel-based morphometry -- the methods. NeuroImage, 11, 805–821. doi:10.1006/nimg.2000.0582 [PubMed: 10860804]

Bassett DS, & Bullmore ET (2017). Small-world brain networks revisited. The Neuroscientist, 23, 499–516. doi:10.1177/1073858416667720 [PubMed: 27655008]

Blei DM, Ng AY, & Jordan MI (2003). Latent Dirichlet Allocation. Journal of Machine Learning Research, 3, 993–1022. doi:10.1162/jmlr.2003.3.4-5.993

Braak H, & Braak E (1991). Neuropathological stageing of Alzheimer-related changes. Acta Neuropathologica, 82(4), 239–59. [PubMed: 1759558]

Braak H, & Braak E (1996). Evolution of the neuropathology of Alzheimer's disease. Acta Neurologica Scandinavica, 94, 3–12. doi:10.1111/j.1600-0404.1996.tb05866.x

Braak H, Braak E, & Bohl J (1993). Staging of Alzheimer-related cortical destruction. European Neurology, 33, 403–408. doi: 10.1159/000116984 [PubMed: 8307060]

Byun MS, Kim SE, Park J, Yi D, Choe YM, Sohn BK, … Lee DY (2015). Heterogeneity of regional brain atrophy patterns associated with distinct progression rates in Alzheimer's disease. PLoS ONE 10(11): e0142756. doi:10.1371/journal.pone.0142756 [PubMed: 26618360]

Carmichael O, McLaren DG, Tommet D, Mungas D, & Jones RN (2013). Coevolution of brain structures in amnestic mild cognitive impairment. NeuroImage, 66, 449–456. doi:10.1016/j.neuroimage.2012.10.029 [PubMed: 23103689]

Decarli C, Maillard P, & Fletcher E (2013). Four Tissue Segmentation in ADNI II. Retrieved from http://adni.loni.usc.edu/methods/mri-tool/

Fair DA, Cohen AL, Dosenbach NUF, Church JA, Miezin FM, Barch DM, … Schlaggar BL (2008). The maturing architecture of the brain's default network. Proceedings of the National Academy of Sciences. doi:10.1073/pnas.0800376105

Fischl B (2012). FreeSurfer. NeuroImage. doi:10.1016/j.neuroimage.2012.01.021

Fletcher E (2014). Using prior information to enhance sensitivity of longitudinal brain change computation. In Chen CH (Ed.), Frontiers of medical imaging (pp. 63–81). Hackensack, NJ: World Scientific.

Fletcher E, Gavett B, Harvey D, Farias S, Olichney J, Beckett L, … Mungas D (2018). Brain volume change and cognitive trajectories in aging. Neuropsychology, 32(4). doi:10.1037/neu0000447

Author Manuscript Author Manuscript Author Manuscript Author Manuscript

Fletcher E, Knaack A, Singh B, Lloyd E, Wu E, Carmichael O, … Alzheimer's Disease Neuroimaging Initiative. (2013). Combining boundary-based methods with tensor-based morphometry in the measurement of longitudinal brain change. IEEE Transactions on Medical Imaging, 32(2), 223–236. doi:10.1109/TMI.2012.2220153 [PubMed: 23014714]

Fletcher E, Singh B, Harvey D, Carmichael O, & DeCarli C (2012). Adaptive image segmentation for robust measurement of longitudinal brain tissue change. In 2012 annual international conference of the ieee engineering in medicine and biology society (Vol. 2012, pp. 5319–5322). IEEE. doi:10.1109/EMBC.2012.6347195

Fletcher E, Villeneuve S, Maillard P, Harvey D, Reed B, Jagust W, & DeCarli C (2016). Beta-amyloid, hippocampal atrophy and their relation to longitudinal brain change in cognitively normal individuals. Neurobiology of Aging, 40, 173–180. doi:10.1016/j.neurobiolaging.2016.01.133 [PubMed: 26973117]

Fjell AM, McEvoy L, Holland D, Dale AM, & Walhovd KB (2014). What is normal in normal aging? Effects of aging, amyloid and Alzheimer's disease on the cerebral cortex and the hippocampus. Progress in Neurobiology, 117, 20–40. doi:10.1016/j.pneurobio.2014.02.004 [PubMed: 24548606]

Fjell A, Walhovd KB, Fennema-Notestine C, McEvoy LK, Hagler DJ, Holland D, … Dale AM (2009). One-year brain atrophy evident in healthy aging. The Journal of Neuroscience, 29, 15223–15231. doi:10.1523/JNEUROSCI.3252-09.2009 [PubMed: 19955375]

Gavett B, Fletcher E, Harvey D, Farias S, Olichney J, Beckett L, … Mungas D (2018). Ethnoracial differences in brain structure change and cognitive change. Neuropsychology, 32(5). doi:10.1037/neu0000452

Hinton L, Carter K, Reed BR, Beckett L, Lara E, DeCarli C, & Mungas D (2010). Recruitment of a Community-based Cohort for Research on Diversity and Risk of Dementia. Alzheimer Disease & Associated Disorders, 24(3), 1. doi:10.1097/WAD.0b013e3181c1ee01 [PubMed: 19571730]

Hu L, & Bentler PM (1999). Cutoff criteria for fit indexes in covariance structure analysis: Conventional criteria versus new alternatives. Structural Equation Modeling: A Multidisciplinary Journal, 6(1), 1–55. doi:10.1080/10705519909540118

Iaccarino L, Tammewar G, Ayakta N, Baker SL, Bejanin A, Boxer AL, … Rabinovici GD (2018). Local and distant relationships between amyloid, tau and neurodegeneration in Alzheimer's Disease. NeuroImage: Clinical, 17, 452–464. doi:10.1016/j.nicl.2017.09.016 [PubMed: 29159058]

Klein A, & Tourville J (2012). 101 labeled brain images and a consistent human cortical labeling protocol. Frontiers in Neuroscience. doi:10.3389/fnins.2012.00171

Kochunov P, Lancaster JL, Thompson P, Woods R, Mazziotta J, Hardies J, & Fox P (2001). Regional spatial normalization: toward an optimal target. Journal of Computer Assisted Tomography, 25(5), 805–816. [PubMed: 11584245]

Lee DY, Fletcher E, Martinez O, Zozulya N, Kim J, Tran J, … DeCarli C (2010). Vascular and Degenerative Processes Differentially Affect Regional Interhemispheric Connections in Normal Aging, Mild Cognitive Impairment, and Alzheimer Disease. Stroke, 41(8), 1791–1797. doi:10.1161/STROKEAHA.110.582163 [PubMed: 20595668]

Mak E, Su L, Williams GB, Watson R, Firbank M, Blamire AM, & O'Brien JT (2015). Longitudinal assessment of global and regional atrophy rates in Alzheimer's disease and dementia with Lewy bodies. NeuroImage: Clinical, 7, 456–462. 10.1016/j.nicl.2015.01.017 [PubMed: 25685712]

McArdle JJ, Hamgami F, Jones K, Jolesz F, Kikinis R, Spiro III A, & Albert MS (2004). Structural modeling of dynamic changes in memory and brain structure using longitudinal data from the normative aging study. Journals of Gerontology: Psychological Sciences, 59B, P294–P304.

McKhann G, Drachman D, Folstein M, Katzman R, Price D, & Stadlan EM (1984). Clinical diagnosis of Alzheimer's disease: Report of the NINCDS-ADRDA Work Group* under the auspices of Department of Health and Human Services Task Force on Alzheimer's Disease. Neurology. doi:10.1212/WNL.34.7.939

McKhann GM, Knopman DS, Chertkow H, Hyman BT, Jack CR, Kawas CH, … Phelps CH (2011). The diagnosis of dementia due to Alzheimer's disease: Recommendations from the National Institute on Aging-Alzheimer's Association workgroups on diagnostic guidelines for Alzheimer's disease. doi:10.1016/j.jalz.2011.03.005

Author Manuscript Author Manuscript Author Manuscript Author Manuscript

Mesulam M-M (2000). Behavioral neuroanatomy: Large-scale networks, association cortex, frontal syndromes, the limbic system, and hemispheric specializations. In Mesulam M-M (Ed.). Principles of Behavioral and Cognitive Neurology, 1–120. New York: Oxford University Press.

Mungas D, Harvey D, Reed BR, Jagust WJ, DeCarli C, Beckett L, … Chui HC (2005). Longitudinal volumetric MRI change and rate of cognitive decline. Neurology, 65(4), 565–571. doi:10.1212/01.wnl.0000172913.88973.0d [PubMed: 16116117]

Mungas DM, Reed BR, Marshall SC, & González HM (2000). Development of psychometrically matched English and Spanish language neuropsychological tests for older persons. Neuropsychology, 14(2), 209–223. [PubMed: 10791861]

Mungas D, Reed BR, Crane PK, Haan MN, & González H (2004). Spanish and English Neuropsychological Assessment Scales (SENAS): Further development and psychometric characteristics. Psychological Assessment, 16(4), 347–359. doi:10.1037/1040-3590.16.4.347 [PubMed: 15584794]

Mungas D, Reed BR, Haan MN, & González H (2005a). Spanish and English Neuropsychological Assessment Scales: Relationship to demographics, language, cognition, and independent function. Neuropsychology, 19(4), 466–475. doi:10.1037/0894-4105.19.4.466 [PubMed: 16060821]

Mungas D, Reed BR, Tomaszewski Farias S, & DeCarli C (2005b). Criterion-referenced validity of a neuropsychological test battery: Equivalent performance in elderly Hispanics and non-Hispanic Whites. Journal of the International Neuropsychological Society, 11(5), 620–630. doi:10.1017/S1355617705050745 [PubMed: 16212690]

Murray ME, Graff-Radford NR, Ross OA, Petersen RC, Duara R, & Dickson DW (2011). Neuropathologically defined subtypes of Alzheimer's disease with distinct clinical characteristics: A retrospective study. Lancet Neurology, 10(9), 785–796. doi:10.1016/S1474-4422(11)70156-9 [PubMed: 21802369]

Muthén LK, & Muthén BO (1998). Mplus User's Guide. Los Angeles: Muthén & Muthén.

Mwangi B, Tian TS, & Soares JC (2014). A review of feature reduction techniques in neuroimaging. Neuroinformatics, 12, 229–244. doi:10.1007/s12021-013-9204-3 [PubMed: 24013948]

Nichols TE, & Holmes AP (2002). Nonparametric permutation tests for functional neuroimaging: A primer with examples. Human Brain Mapping, 15(1), 1–25. doi:10.1002/hbm.1058 [PubMed: 11747097]

Ossenkoppele R, Cohn-Sheehy BI, La Joie R, Vogel JW, Möller C, Lehmann M, … Rabinovici GD (2015). Atrophy patterns in early clinical stages across distinct phenotypes of Alzheimer's disease. Human Brain Mapping, 36, 4421–4437. doi:10.1002/hbm.22927 [PubMed: 26260856]

Persson K, Eldholm RS, Barca ML, Cavallin L, Ferreira D, Knapskog A-B, … Engedal K (2017) MRI-assessed atrophy subtypes in Alzheimer's disease and the cognitive reserve hypothesis. PLoS ONE 12(10): e0186595. doi:10.1371/journal.pone.0186595 [PubMed: 29036183]

Persson N, Ghisletta P, Dahle CL, Bender AR, Yang Y, Yuan P, Daugherty AM, & Raz N (2016). Regional brain shrinkage and change in cognitive performance over two years: The bidirectional influences of brain and cognitive reserve factors. NeuroImage, 126, 15–26. doi:10.1016/j.neuroimage.2015.11.028 [PubMed: 26584866]

Raz N, Lindenberger U, Rodrigue KM, Kennedy KM, Head D, Williamson A … Acker JD (2005). Regional brain changes in aging health adults: General trends, individual differences, and modifiers. Cerebral Cortex, 15, 1676–1689. doi:10.1093/cercor/bhi044 [PubMed: 15703252]

Rueckert D, Aljabar P, Heckemann RA, Hajnal JV, & Hammers A (2006). Diffeomorphic Registration Using B-Splines. In (pp. 702–709). Springer, Berlin, Heidelberg. doi:10.1007/11866763_86

Schwarz G (1978). Estimating the Dimension of a Model. The Annals of Statistics, 6(2), 461–464. doi:10.1214/aos/1176344136

Sclove SL (1987). Application of model-selection criteria to some problems in multivariate analysis. Psychometrika, 52(3), 333–343. doi:10.1007/BF02294360

Seeley WW, Crawford RK, Zhou J, Miller BL, & Greicius MD (2009). Neurodegenerative Diseases Target Large-Scale Human Brain Networks. Neuron. doi:10.1016/j.neuron.2009.03.024

VandenHeuvel MP, & Sporns O (2011). Rich-club organization of the human connectome. Journal of Neuroscience. doi:10.1523/JNEUROSCI.3539-11.2011

Author Manuscript Author Manuscript Author Manuscript Author Manuscript

Vernet M, Quentin R, Chanes L, Mitsumasu A, & Valero-Cabré A (2014). Frontal eye field, where art thou? Anatomy, function, and non-invasive manipulation of frontal regions involved in eye movements and associated cognitive operations. Frontiers in Integrative Neuroscience. doi:10.3389/fnint.2014.00066

Vossel S, Geng JJ, & Fink GR (2014). Dorsal and ventral attention systems: Distinct neural circuits but collaborative roles. Neuroscientist. doi:10.1177/1073858413494269

Whitwell JL, Dickson DW, Murray ME, Weigand SD, Tosakulwong N, Senjem ML, … Josephs KA (2012). Neuroimaging correlates of pathologically defined subtypes of Alzheimer's disease: A case-control study. Lancet Neurology, 11(10), 868–877. doi:10.1016/S1474-4422(12)70200-4 [PubMed: 22951070]

Winblad B, Palmer K, Kivipelto M, Jelic V, Fratiglioni L, Wahlund LO, … Petersen RC (2004). Mild cognitive impairment - Beyond controversies, towards a consensus: Report of the International Working Group on Mild Cognitive Impairment. Journal of Internal Medicine. doi:10.1111/j.1365-2796.2004.01380.x

Zhang X, Mormino EC, Sun N, Sperling RA, & Sabuncu MR, Yeo BTT (2016). Bayesian model reveals latent atrophy factors with dissociable cognitive trajkcctories in Alzheimer's disease. Proceedings of the National Academy of Sciences, 113, E6535–E6544. doi:10.1073/pnas.1611073113

Author Manuscript Author Manuscript Author Manuscript Author Manuscript

Key Points

Question:

Are there patterns of coordinated regional brain changes that underlie aging-associated changes in cognitive functioning?

Findings:

In addition to global brain atrophy, four specific factors underlying regional brain atrophy (corresponding to volume changes in prefrontal association cortex, posterior association cortex, temporolimbic areas, and medial temporal lobes) are dissociable from one another; three of these (global, temporolimbic, and medial temporal) exert a strong influence over global cognitive decline.

Importance:

These findings allow us to reduce dozens of brain volume measurements into a smaller number of elements that (1) represent systematic patterns of change in cortical ROI volumes and (2) explain 59% of the variance in aging-associated cognitive decline.

Next Steps:

The identification of a well-fitting model that can jointly explain changes in brain volume and cognition allows for continued advances in understanding the mechanisms responsible for conferring risk of or resilience to late-life cognitive decline and dementia.

Author Manuscript Author Manuscript Author Manuscript Author Manuscript

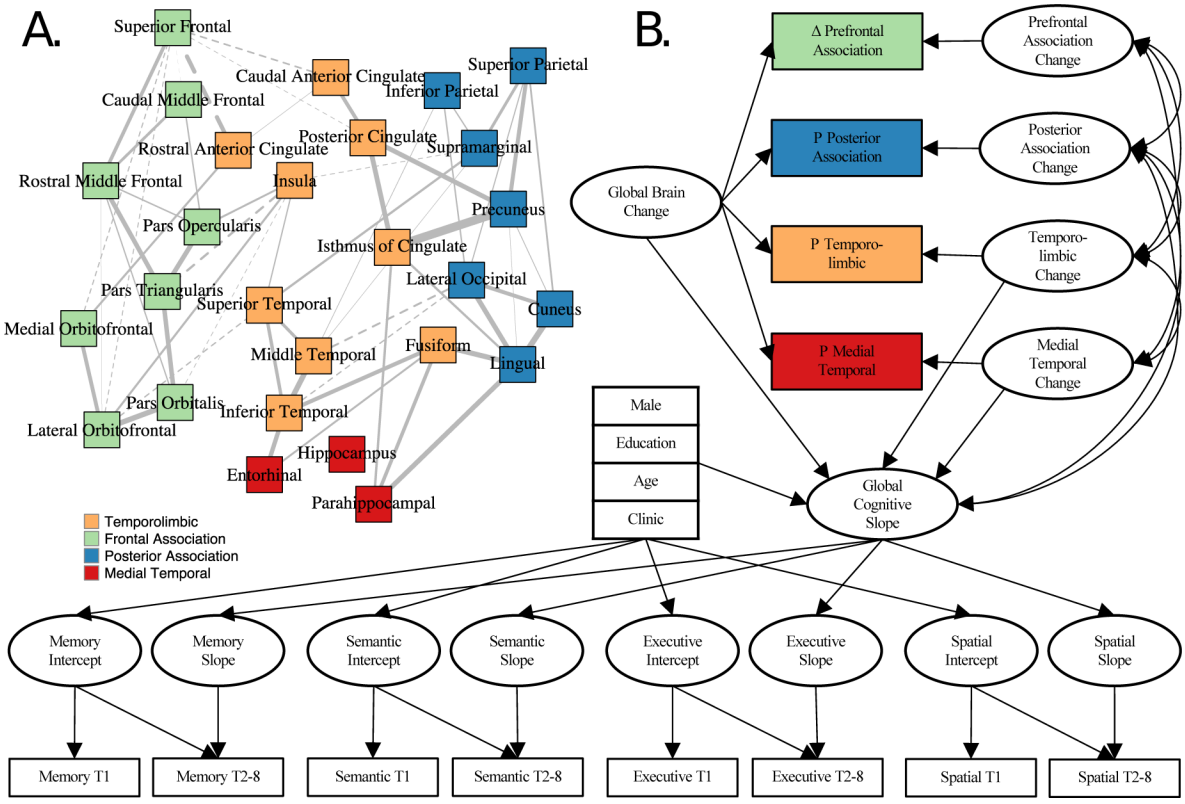

Figure 1.

Graphical depiction of Model 3, the preferred model for explaining coordinated changes in brain volume and cognition. (A.) shows a network graph representing our approach to modelling the residual covariances between indicator ROIs. Vertices (squares) represent bilateral ROIs from the Mindboggle atlas plus a separate ROI for the hippocampus. Vertices are color coded by latent factor. Edges (gray lines) represent adjacent brain regions that were allowed to share residual covariance (variance shared between ROIs that is not explained by the brain change factors). Solid lines represent positive residual correlations and dashed lines represent negative residual correlations. Line thickness is proportional to the strength of the residual correlation. Because the hippocampus was parcellated independent of the other ROIs, no residual covariance was modelled between the hippocampus and its adjacent structures. The magnitude and direction of these residual correlations can be interpreted as the strength of association between two adjacent regions after accounting for the influence of the latent change factors for which the ROIs serve as indicators. (B.) shows a path diagram depicting the general modelling framework used to identify brain change factors and their relations with cognitive change. Not shown are correlations of the cognitive intercepts with one another, with the demographic covariates, with the brain change factors, and with the global cognitive slope.

Author Manuscript Author Manuscript Author Manuscript Author Manuscript

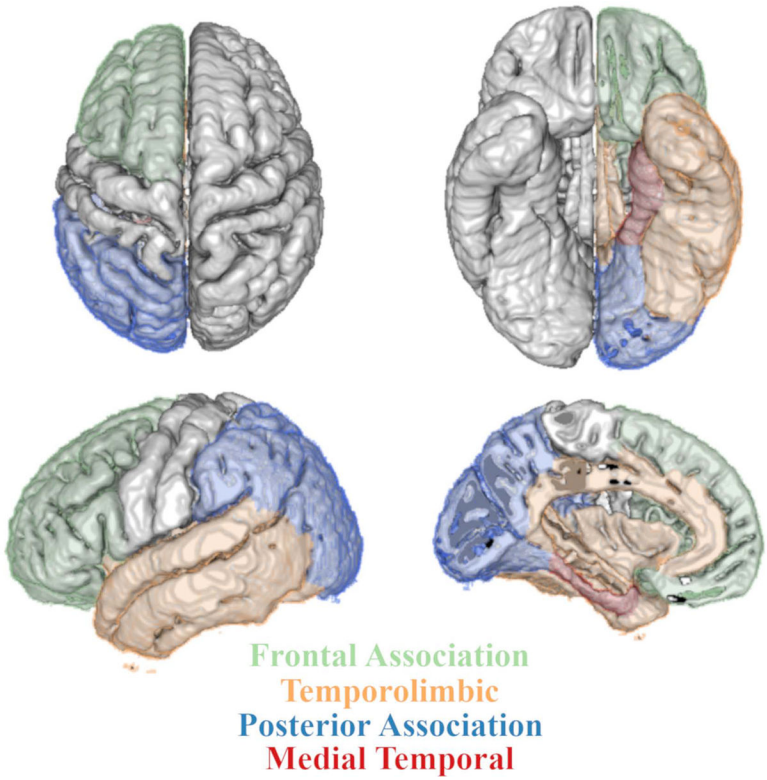

Figure 2.

3D surface map of brain change factors and their associations with global cognitive slope. Left hemisphere regions are color coded according to the four brain change group factors identified in the current study.

Author Manuscript Author Manuscript Author Manuscript Author Manuscript

Table 1.

Baseline Participant Demographics and Cognitive Performance Scores

N	358
Study visits (n); *M* (SD)	6.72 (3.01)
MRI scans (n); M (SD)	2.69 (0.87)
Inter-scan interval (years); M (SD)	5.47 (2.99)
Age (years); *M* (SD)	74.81 (7.17)
Education (years); *M* (SD)	13.46 (4.41)
Female sex; n (%)	216 (60.3%)
Spanish language; n (%)	46 (12.9%)
Race/Ethnicity; n (%)	
African American	79 (22.1%)
Hispanic	90 (25.1%)
White	170 (47.5%)
Other	18 (5.0%)
Missing	1 (0.3%)
Clinic Recruitment; n (%)	85 (23.7%)
Clinical Diagnosis; n (%)	
Missing	12 (3.4%)
Dementia	20 (5.6%)
MCI	115 (32.1%)
Normal	211 (58.9%)
Global CDR; n (%)	
0	147 (41.1%)
0.5	148 (41.3%)
1	21 (5.9%)
Missing	42 (11.7%)
MMSE; *M* (SD)	27.17 (2.77)
SENAS Verbal Memory; *M* (SD)	0.15 (0.85)
SENAS Semantic Memory; *M* (SD)	0.06 (0.85)
SENAS Executive Functioning; *M* (SD)	0.21 (0.84)
SENAS Spatial; *M* (SD)	0.12 (0.97)

Note. MRI = magnetic resonance imaging; MCI = mild cognitive impairment; CDR = Clinical Dementia Rating; MMSE = Mini-Mental State Examination; SENAS = Spanish and English Neuropsychological Assessment Scales.

Author Manuscript Author Manuscript Author Manuscript Author Manuscript

Table 2.

Description of Brain Change Measurement Models

ROI	Model 1[a]	Model 2[b]	Model 3[c]	Model 4
Caudal Anterior Cingulate	Prefrontal	Temporolimbic	Temporolimbic	Global
Caudal Middle Frontal	Prefrontal	Frontal	Prefrontal	Global
Cuneus	Sensory	Occipital	Posterior Association	Global
Entorhinal	DMN+MTL	Temporolimbic	MTL	Global
Fusiform	DMN+MTL	Temporolimbic	Temporolimbic	Global
Hippocampus	DMN+MTL	Temporolimbic	MTL	Global
Inferior Parietal	DMN+MTL	Parietal	Posterior Association	Global
Inferior Temporal	DMN+MTL	Temporolimbic	Temporolimbic	Global
Insula	DMN+MTL	Temporolimbic	Temporolimbic	Global
Isthmus of Cingulate	DMN+MTL	Temporolimbic	Temporolimbic	Global
Lateral Occipital	Sensory	Occipital	Posterior Association	Global
Lateral Orbitofrontal	Prefrontal	Frontal	Prefrontal	Global
Lingual	DMN+MTL	Occipital	Posterior Association	Global
Medial Orbitofrontal	Prefrontal	Frontal	Prefrontal	Global
Middle Temporal	DMN+MTL	Temporolimbic	Temporolimbic	Global
Paracentral	Sensory	Frontal	–	Global
Parahippocampus	DMN+MTL	Temporolimbic	MTL	Global
Pars Opercularis	Prefrontal	Frontal	Prefrontal	Global
Pars Orbitalis	Prefrontal	Frontal	Prefrontal	Global
Pars Triangularis	Prefrontal	Frontal	Prefrontal	Global
Pericalcarine	–	Occipital	–	Global
Postcentral	Sensory	Parietal	–	Global
Posterior Cingulate	DMN+MTL	Temporolimbic	Temporolimbic	Global
Precentral	Prefrontal	Frontal	–	Global
Precuneus	DMN+MTL	Parietal	Posterior Association	Global
Rostral Anterior Cingulate	Prefrontal	Temporolimbic	Temporolimbic	Global
Rostral Middle Frontal	Prefrontal	Frontal	Prefrontal	Global
Superior Frontal	Prefrontal	Frontal	Prefrontal	Global

Neuropsychology. Author manuscript; available in PMC 2022 September 01.

Author Manuscript Author Manuscript Author Manuscript Author Manuscript

ROI	Model 1[a]	Model 2[b]	Model 3[c]	Model 4
Superior Parietal	Sensory	Parietal	Posterior Association	Global
Superior Temporal	DMN+MTL	Temporolimbic	Temporolimbic	Global
Supramarginal	DMN+MTL	Parietal	Posterior Association	Global
Transverse Temporal	Prefrontal	Temporolimbic	–	Global

Note. The first three models contain a global factor (bifactor structure) with model-specific indicators as shown. The fourth model is a single factor model. DMN = default mode network; MTL = medial temporal lobe.

[a] Inspired by Carmichael et al. (2013), but group factors 1 (posterior DMN) and 3 (MTL) were merged due to a "not positive definite" psi matrix (r = 1.099)

[b] Inspired by Fletcher et al. (2018)

[c] No primary sensory/motor cortex included in the model

Author Manuscript Author Manuscript Author Manuscript Author Manuscript

Table 3.

Model Fit Statistics for Structural Models Regressing Cognitive Change onto Brain Change

Model	CFI	TLI	RMSEA	SRMR
Model 1	0.879	0.869	0.061 [0.059, 0.064]	0.081
Model 2	0.899	0.890	0.056 [0.054, 0.059]	0.069
Model 3	**0.927**	**0.920**	**0.049 [0.047, 0.052]**	**0.063**
Model 4	0.849	0.839	0.068 [0.066, 0.070]	0.089

Note. CFI = comparative fit index; RMSEA = root mean square error of approximation; SRMR = standardized root mean square residual. Bold text = most preferable model fit statistics.

Neuropsychology. Author manuscript; available in PMC 2022 September 01.

Author Manuscript Author Manuscript Author Manuscript Author Manuscript

Table 4.

Standardized Factor Loadings (SE) of Change in 27 MRI Regions of Interest onto Five Brain Change Factors (Derived from Model 3)

Region of Interest	Global	Temporolimbic	Medial Temporal	Prefrontal	Posterior Association
Rostral Anterior Cingulate	0.192 (0.103)	0.915 (0.022)			
Caudal Anterior Cingulate	0.229 (0.099)	0.837 (0.032)			
Insula	0.472 (0.084)	0.717 (0.052)			
Posterior Cingulate	0.455 (0.081)	0.660 (0.054)			
Middle Temporal	0.769 (0.062)	0.566 (0.078)			
Superior Temporal	0.733 (0.062)	0.546 (0.074)			
Inferior Temporal	0.710 (0.062)	0.528 (0.074)			
Isthmus of Cingulate	0.472 (0.084)	0.493 (0.074)			
Fusiform	0.809 (0.051)	0.467 (0.081)			
Parahippocampal	0.684 (0.060)		0.697 (0.059)		
Hippocampus	0.492 (0.058)		0.627 (0.042)		
Entorhinal	0.581 (0.054)		0.547 (0.059)		
Superior Frontal	−0.059 (0.107)			0.940 (0.018)	
Rostral Middle Frontal	0.044 (0.102)			0.891 (0.017)	
Caudal Middle Frontal	0.098 (0.103)			0.862 (0.022)	
Pars Opercularis	0.285 (0.097)			0.843 (0.033)	
Pars Triangularis	0.186 (0.096)			0.823 (0.026)	
Medial Orbitofrontal	0.290 (0.092)			0.786 (0.036)	
Lateral Orbitofrontal	0.398 (0.074)			0.606 (0.050)	
Pars Orbitalis	0.270 (0.071)			0.500 (0.036)	
Superior Parietal	0.245 (0.091)				0.851 (0.024)
Supramarginal	0.505 (0.082)				0.774 (0.049)
Precuneus	0.553 (0.076)				0.752 (0.053)
Inferior Parietal	0.571 (0.069)				0.711 (0.051)
Lingual	0.547 (0.064)				0.477 (0.061)
Cuneus	0.419 (0.059)				0.415 (0.055)
Lateral Occipital	0.831 (0.028)				0.185 (0.077)

Author Manuscript Author Manuscript Author Manuscript Author Manuscript

Table 5.

Standardized Parameter Estimates for Associations Between Cognitive Change and Brain Change (Derived from Model 3)

Factor 1	Operator	Factor 2	est	SE	95% HDI
Global Slope	ON	Global Brain	0.434*	0.070	[0.290, 0.563]
Global Slope	ON	Temporolimbic	0.275*	0.085	[0.110, 0.443]
Global Slope	ON	Medial Temporal	0.240*	0.085	[0.073, 0.407]
Global Slope	WITH	Prefrontal	−0.121*	0.046	[−0.212, −0.034]
Global Slope	WITH	Posterior Association	−0.227*	0.052	[−0.331, −0.126]
Temporolimbic	WITH	Medial Temporal	0.716*	0.054	[0.607, 0.810]
Temporolimbic	WITH	Prefrontal	0.904*	0.020	[0.863, 0.940]
Temporolimbic	WITH	Posterior Association	0.750*	0.043	[0.666, 0.830]
Medial Temporal	WITH	Prefrontal	0.577*	0.068	[0.440, 0.700]
Medial Temporal	WITH	Posterior Association	0.435*	0.088	[0.256, 0.593]
Prefrontal	WITH	Posterior Association	0.883*	0.023	[0.836, 0.925]

Note. HDI = highest density interval.

*$p < .05$.